

# Distillation of Liquid Xenon to Remove Krypton

K. Abe<sup>a</sup>, J. Hosaka<sup>a</sup>, T. Iida<sup>a</sup>, M. Ikeda<sup>a</sup>, K. Kobayashi<sup>a</sup>,  
 Y. Koshio<sup>a</sup>, A. Minamino<sup>a</sup>, M. Miura<sup>a</sup>, S. Moriyama<sup>a</sup>,  
 M. Nakahata<sup>a,c,\*</sup>, Y. Nakajima<sup>a</sup>, T. Namba<sup>a,1</sup>, H. Ogawa<sup>a</sup>,  
 H. Sekiya<sup>a</sup>, M. Shiozawa<sup>a</sup>, Y. Suzuki<sup>a,c</sup>, A. Takeda<sup>a</sup>,  
 Y. Takeuchi<sup>a</sup>, K. Ueshima<sup>a</sup>, M. Yamashita<sup>a</sup>, K. Kaneyuki<sup>b</sup>,  
 Y. Ebizuka<sup>d</sup>, J. Kikuchi<sup>d</sup>, A. Ota<sup>d</sup>, S. Suzuki<sup>d</sup>, T. Takahashi<sup>d</sup>,  
 H. Hagiwara<sup>e</sup>, T. Kamei<sup>e</sup>, K. Miyamoto<sup>e</sup>, T. Nagase<sup>e</sup>,  
 S. Nakamura<sup>e</sup>, Y. Ozaki<sup>e</sup>, T. Sato<sup>e</sup>, Y. Fukuda<sup>f</sup>, T. Sato<sup>f</sup>,  
 K. Nishijima<sup>g</sup>, M. Sakurai<sup>g</sup>, T. Maruyama<sup>g</sup>, D. Motoki<sup>g</sup>,  
 Y. Itow<sup>h</sup>, H. Ohsumi<sup>i</sup>, S. Tasaka<sup>j</sup>, S. B. Kim<sup>k</sup>, Y. D. Kim<sup>l</sup>,  
 J. I. Lee<sup>l</sup>, S. H. Moon<sup>l</sup>, Y. Urakawa<sup>m</sup>, M. Uchino<sup>m</sup>, and  
 Y. Kamioka<sup>m</sup>

for the XMASS Collaboration

<sup>a</sup>*Kamioka Observatory, Institute for Cosmic Ray Research, The University of Tokyo, Kamioka, Hida, Gifu 506-1205, Japan*

<sup>b</sup>*Research Center for Cosmic Neutrinos, Institute for Cosmic Ray Research, The University of Tokyo, Kashiwa, Chiba 277-8582, Japan*

<sup>c</sup>*Institute for the Physics and Mathematics of the Universe, The University of Tokyo, Kashiwa, Chiba 277-8582, Japan*

<sup>d</sup>*Faculty of Science and Engineering, Waseda University, Shinjuku-ku, Tokyo 162-8555, Japan*

<sup>e</sup>*Department of Physics Faculty of Engineering, Yokohama National University, Yokohama, Kanagawa 240-8501, Japan*

<sup>f</sup>*Department of Physics, Miyagi University of Education, Sendai, Miyagi 980-0845, Japan*

<sup>g</sup>*Department of Physics, Tokai University, Hiratsuka, Kanagawa 259-1292, Japan*

<sup>h</sup>*Solar Terrestrial Environment Laboratory, Nagoya University, Nagoya, Aichi 464-8602, Japan*

<sup>i</sup>*Faculty of Culture and Education, Saga University, Honjo, Saga 840-8502, Japan*

<sup>j</sup>*Department of Physics, Gifu University, Gifu, Gifu 501-1193, Japan*

<sup>k</sup>*Department of Physics, Seoul National University, Seoul 151-742, Korea*

<sup>l</sup>*Department of Physics, Sejong University, Seoul 143-747, Korea*

## Abstract

A high performance distillation system to remove krypton from xenon was constructed, and a purity level of  $\text{Kr}/\text{Xe} = \sim 3 \times 10^{-12}$  was achieved. This development is crucial in facilitating high sensitivity low background experiments such as the search for dark matter in the universe.

*Key words:* liquid xenon, krypton removal, dark matter

*PACS:* 29.40.Mc, 81.20.Ym, 95.35.+d

---

## 1 Introduction

Liquid xenon is one of the most attractive materials for use in detectors for astroparticle and particle physics [1,2,3,4,5]. As a scintillator it has a large light yield, comparable to that of NaI(Tl), and can be used for detectors with low energy thresholds and high energy resolution. Because of the high atomic number of xenon ( $Z = 54$ ) and its high density in liquid form ( $\sim 3 \text{ g/cm}^3$ ), it contributes to reduction of the environmental background, such as  $\gamma$ -rays and  $\beta$ -rays from uranium and thorium contamination, by self-shielding. Another big advantage of liquid xenon is that xenon does not have long-lived radioactive isotopes, and thus experiments on rare phenomena (such as dark matter searches and double beta decay experiments) may be carried out shortly after moving the xenon underground from the surface.

One drawback of liquid xenon is the possibility of contamination with radioactive  $^{85}\text{Kr}$ . Xenon is usually produced from air. The concentration of xenon in air is  $\sim 10^{-7}$  mol/mol, while the concentration of krypton is  $\sim 10^{-6}$  mol/mol. In the commercial production of xenon, krypton is removed by distillation or adsorption. But, the commercially available xenon contains  $10^{-9} \sim 10^{-6}$  mol/mol of krypton, because the removal starts from the Kr/Xe ratio of about 10 and such purity is enough for most of the applications of xenon.  $^{85}\text{Kr}$  is a radioactive nucleus which decays into rubidium-85 with a half-life of 10.76 years, and emits  $\beta$ -rays with a maximum energy of 687 keV and a 99.57% branching

---

\* Corresponding Author

*Email address:* nakahata@suketto.icrr.u-tokyo.ac.jp (M. Nakahata).

<sup>1</sup> Present address: International Centre for Elementary Particle Physics, the University of Tokyo, Tokyo 113-0033, Japan

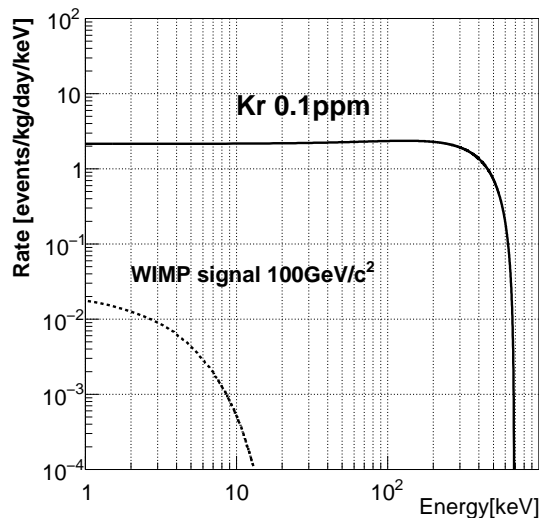


Fig. 1. Background event rate of  $^{85}\text{Kr}$  for a Kr/Xe ratio of  $10^{-7}$  mol/mol, compared with dark matter signal rate, assuming a cross section of  $10^{-7}$  pb and a WIMP mass of  $100 \text{ GeV}/c^2$ . A quenching factor of 0.2 is assumed for the dark matter signal.

ratio. (The remaining 0.43% represents a  $\beta$ -emission with a maximum energy of 173 keV followed by a 514 keV  $\gamma$ -ray emission.) Large quantities of  $^{85}\text{Kr}$  produced artificially as a product of nuclear fission are the main source of  $^{85}\text{Kr}$  in air. The concentration of  $^{85}\text{Kr}$  in air is measured to be  $\sim 1 \text{ Bq}/\text{m}^3$ [6,7], and it corresponds to  $^{85}\text{Kr}/\text{Kr} = \sim 10^{-11}$ . Assuming a Kr/Xe ratio of  $10^{-7}$  mol/mol, the background event rate of  $^{85}\text{Kr}$  is as shown in Fig. 1. ( $^{85}\text{Kr}/\text{Kr}$  of  $1.2 \times 10^{-11}$  is used here.) The expected dark matter event rate is also plotted, assuming a cross section of  $10^{-7}$  pb and a WIMP mass of  $100 \text{ GeV}/c^2$ . A quenching factor of 0.2 is assumed for the dark matter signal.

Because next-generation dark matter detectors aim at a sensitivity of  $10^{-9}$  pb for the dark matter-proton cross section, a background rate of  $10^{-4}$  events/keV/day/kg is required. This corresponds to a Kr/Xe ratio of less than  $\sim 10^{-12}$  mol/mol.

The possible methods to remove krypton from xenon are distillation and adsorption. They are commonly used industrial processes but the systems which satisfy our requirements did not exist. A development of adsorption-based chromatography to achieve low Kr concentration is reported in ref.[8]. In this paper, we describe the development of a distillation system for removing krypton to a purity level of  $10^{-12}$ . In section 2, the design principle is discussed, while in section 3, the setup and operation of the distillation system are described. In section 4, we describe a technique for measuring low levels of krypton in xenon gas, and discuss the results.

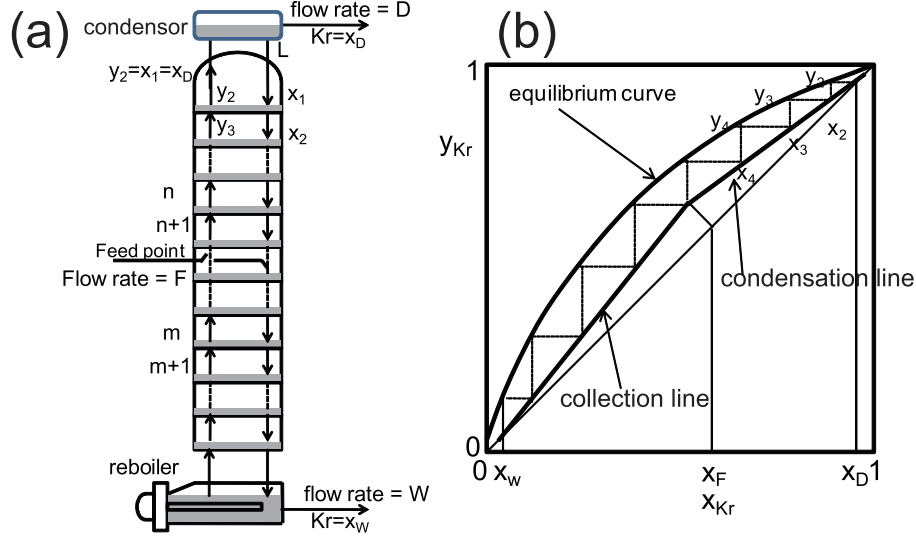


Fig. 2. (a) Illustration of the McCabe-Thiele (M-T) method. The various elements of the figure are explained in the text. (b) Calculation of the number of theoretical cells using the M-T method. The horizontal and vertical axes represent the krypton concentration in the liquid and gas phases, respectively. The thick solid curve is the equilibrium curve, and the thick solid lines are the condensation line and the collection line (details explained in the text).

## 2 Design principle

The boiling point of liquid krypton is 120 K at 1 atmosphere, while that of xenon is 165 K. This means that, in principle, separation of krypton and xenon can be performed by a distillation method. For the basic design of the distillation system, we followed the McCabe-Thiele (M-T) method[9]. It is the standard method of designing a distillation system. At first, the concept of the M-T method is reviewed, and then the application of the method for our purpose is described.

The principle of the M-T method is shown in Fig. 2. The main element in the distillation system is a tower in which gas-liquid equilibrium is maintained. A vessel called a “reboiler”, at the bottom of the tower, boils the liquid using a heater. In order to maintain a constant temperature profile in the tower, a condenser is placed at its top. The supplied xenon gas is cooled down to near boiling point, and then supplied to the feed point in the tower at a flow rate  $F$ , as shown in the figure. The processed xenon, which contains a lower concentration of krypton than the original xenon, is obtained from the reboiler (flow rate  $W$ ), and xenon with a higher krypton concentration is obtained at the top of the tower (flow rate  $D$ ). In the following, the Kr concentration of each xenon is expressed as  $x_F$ ,  $x_W$  and  $x_D$ , respectively. The heating power of the reboiler, which is the same as the cooling power of the condenser at the top of the tower, controls the flow of xenon in the tower (flow rate  $L$ ). The

reflux ratio, represented by  $R = L/D$ , indicates the amount of xenon returned to the tower compared with the amount extracted with a high concentration of krypton.

In the M-T method, the distillation tower is assumed to be a connected series of theoretical cells, with the gas-liquid equilibrium changing by one step in each cell. The number of theoretical cells and the optimal position of the feed point are calculated for given boundary conditions of  $F$ ,  $D$ ,  $W$ ,  $x_F$ ,  $x_W$ ,  $x_D$  and  $R$ .

For an equilibrium of liquid and gas phases in a mixture of elements (in this case, Kr and Xe), the partial pressures of the gas-phase elements (expressed as  $p_{Kr}$  and  $p_{Xe}$ , respectively) can be related to the fraction of each element in the liquid phase (expressed as  $x_{Kr}$  and  $x_{Xe}$ ) by Raoult's law:

$$p_{Kr} = P_{Kr} \cdot x_{Kr} \quad (1)$$

$$p_{Xe} = P_{Xe} \cdot x_{Xe} \quad (2)$$

where  $P_{Kr}$  and  $P_{Xe}$  are the vapor pressures of the corresponding elements (2090 kPa and 201.4 kPa, respectively, at 178 K). Using Raoult's law, the concentrations of Kr in the gas phase ( $y_{Kr}$ ) and the liquid phase ( $x_{Kr}$ ) can be related by the equation

$$y_{Kr} = \frac{\alpha \cdot x_{Kr}}{1 + (\alpha - 1)x_{Kr}} \quad (3)$$

where  $\alpha$  is the ratio of vapor pressures of Kr and Xe,  $P_{Kr}/P_{Xe}$  (10.4 at 178 K). Eq. 3 is called the "equilibrium curve", and it is shown by the thick solid curve in Fig. 2(b). For each theoretical cell, the gas- and liquid-phase Kr concentrations in the neighboring cells are related by conservation of mass flow, and may be expressed as:

$$y_{n+1} = \frac{R}{R+1}x_n + \frac{1}{R+1}x_d \quad (4)$$

$$y_{m+1} = \frac{R'}{R'-1}x_m - \frac{1}{R'-1}x_W \quad (5)$$

where eq. 4 (5) is for the cells above (below) the feeding point, and  $n$  ( $m$ ) is the number of theoretical cells.  $R'$  is  $(L + qF)/W$ , where  $q$  is the fraction of liquid with respect to the total feed material. Equations 4 and 5 represent the "condensation line" and the "collection line", respectively; these are shown as solid lines in Fig. 2(b). Figure 2(b) illustrates the method of estimating the number of required theoretical cells and the optimal feed point.

We designed the distillation tower with the following requirements:

- The Kr concentration of the processed xenon should be three orders of magnitude smaller than that of the original xenon sample, i.e.  $x_W = \frac{1}{1000} \times x_F$ .
- The collection efficiency of xenon should be 99%, i.e.  $W/F = 0.99$  and  $D/F = 0.01$ .
- The system should have a process speed of 0.6 kg Xe per hour, which allows 100 kg xenon to be purified within a week.
- The system should have a reflux ratio of  $R = 20$ , which means the heating power required for the reboiler is 3.3 W.
- Xenon should be fed into the system in the liquid phase, i.e.  $q = 1$ .

A M-T diagram based on these requirements is shown in Fig. 3, in which the concentration of Kr in Xe( $x_F$ ) was assumed to be  $1 \times 10^{-7}$ ; however, the relative locations of the equilibrium, condensation and collection lines do not change significantly even if we assume a lower  $x_F$ . The M-T diagram shows that we need 13 stages of theoretical cells and that the third stage is the optimal location for the xenon feed.

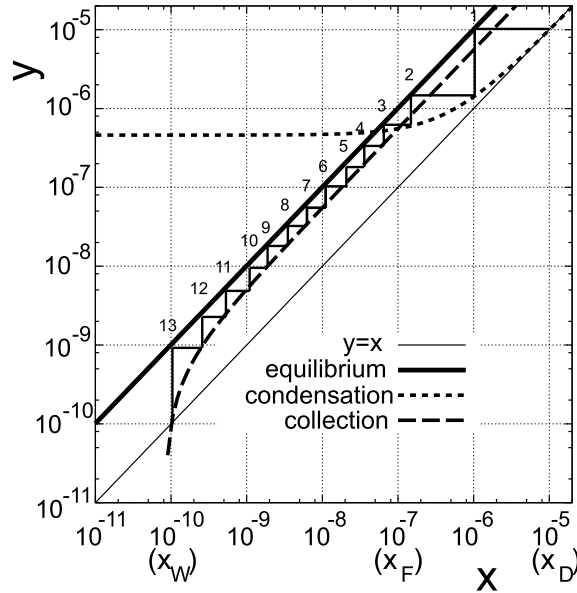


Fig. 3. M-T diagram with system requirements.

### 3 Setup and operation of the distillation system

A key element of the distillation system is the packing column in the distillation tower. We used the “DX laboratory packing” (Sulzer Co.) with a diameter of 2 cm. The catalog specifications of the packing included a liquid load (defined as the flow per unit area per unit time) between 0.1 and 5  $m^3/m^2h$ . In

our case, the liquid loads are 0.13 and 1.2  $m^3/m^2h$  for reflux ratios  $R$  of 20 and 190, respectively. According to the catalog, the length of packing which corresponds to one theoretical cell for a typical liquid (the value for xenon is not given) is about 5 cm. However, the length strongly depends on the liquid load and the type of liquid used. We conservatively increased the length by a factor of three to give a theoretical cell length of 15 cm. (A factor of three is often used in the design of real distillation systems.) As described in the previous section, 13 stages are required to achieve a 1000-fold reduction in krypton concentration. Thus, the total packing length in the distillation tower was set at 208 cm. The optimal position of the feed point was estimated (as described in the previous section) to be the third cell from the top. However, since the length of the theoretical cell depends strongly on various conditions, we shifted the position of the feed to 10.8 cm from the top. This may deviate from the optimal conditions, but a longer distance from the feed point to the extraction point at the bottom allows for the real length of a theoretical cell to be greater than expected.

The full setup of the distillation system is shown in Fig. 4. Before entering the

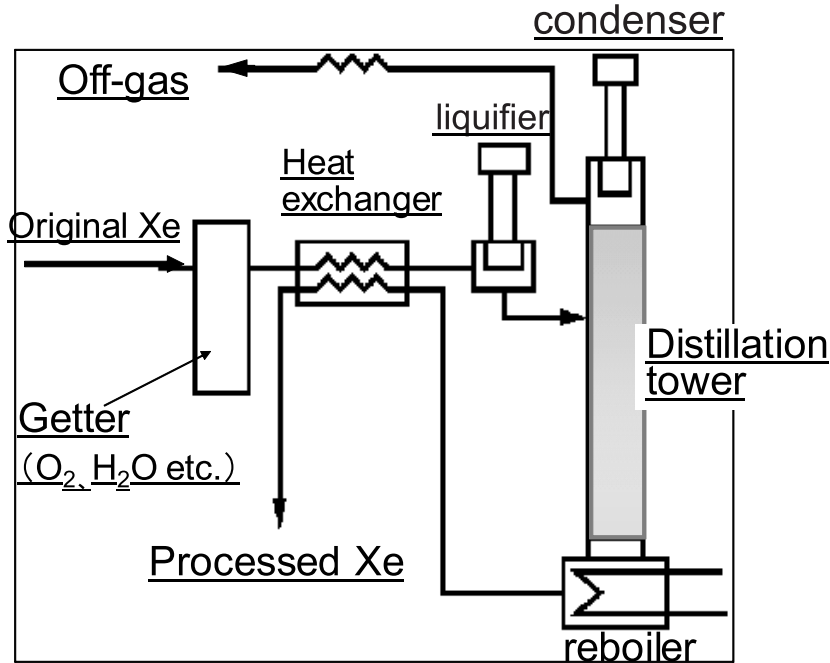


Fig. 4. Flow chart of distillation system.

distillation apparatus, the xenon flows through a getter SPRG-100H-00030X (Taiyo Toyo Sanso Co.), which is able to decrease concentrations of N<sub>2</sub>, CH<sub>4</sub>, O<sub>2</sub>, CO<sub>2</sub>, and CO to below  $1 \times 10^{-10}$  mol/mol, and H<sub>2</sub> and H<sub>2</sub>O below  $5 \times 10^{-10}$  mol/mol. The xenon then flows through a heat exchanger which pre-cools the xenon. For this purpose, the purified xenon gas extracted from the distillation

apparatus is used as a cooling medium. After cooling, the xenon is liquefied by a GM-type refrigerator (TZ-65; Taiyo Nippon Sanso Co.) which has a cooling power of 100 W at around 180 K, and the liquefied xenon is fed into the distillation tower. The temperature of the condenser at the top of the distillation tower is kept at 178 K by an electrical heater. The reboiler is a cylindrical copper vessel with a 200 mm diameter. Three liquid level sensors are placed in the reboiler at 5 mm ( $LL$  level), 20 mm ( $L$  level) and 65 mm ( $H$  level), corresponding to 0.47 kg, 1.88 kg and 6.1 kg of xenon, respectively. For real operation, the heater attached to the reboiler is set to 30 W rather than the value calculated in the conceptual design (3.3 W) in order to ensure better distillation performance with a higher reflux ratio. The purified xenon (low Kr concentration) is collected from the reboiler and goes to a collection bottle via the heat exchanger. Xenon with a high Kr concentration, which is called the “off-gas”, is collected from the top of the distillation tower. The purified and off-gas xenon were collected in stainless steel bottles which were cooled by liquid nitrogen.

The apparatus was used from March 9 to 17, 2004, to process 100 kg of xenon. First, about 2.0 kg of xenon were liquefied and supplied to the distillation tower up to liquid level  $L$  in the reboiler. The heater in the reboiler and the condenser at the top of the distillation tower were switched on, and the system was maintained for 11 hours without collecting purified and off-gas xenon in order to establish the initial gas-liquid equilibrium in the tower. After this time, the flow rate of the purified xenon was set to 0.6 kg/h (1.7 L/min gas flow), and that of the off-gas xenon was set to 0.006 kg/h (17 mL/min). The flow rate of the xenon feed was set at around 0.6 kg/h (1.7 L/min) in the following manner: after the liquid level in the reboiler had reached  $L$ , the rate was set to 0.72 kg/h (2.0 L/min) for about four hours, and then to 0.48 kg/h (1.4 L/min) until the xenon in the reboiler returned to level  $L$ . When we found that the liquid level around  $L$  could be measured more precisely by the monitored pressure of the purified xenon, the flow rate of the xenon feed was fine-tuned to balance the output flow. Figure 5 shows the time variation for off-gas, input and purified xenon. Figure 6 shows the temperature variation as a function of time for the condenser in the distillation tower, the reboiler and the center position in the tower. The temperature was stable to within  $\pm 0.5$  K during the operation. The pressure in the distillation tower was approximately 0.105 MPa (gauge) throughout the operation.

#### 4 Measurement of krypton concentration

In this section we describe the measurement of Kr concentration in input, off-gas and purified xenon.



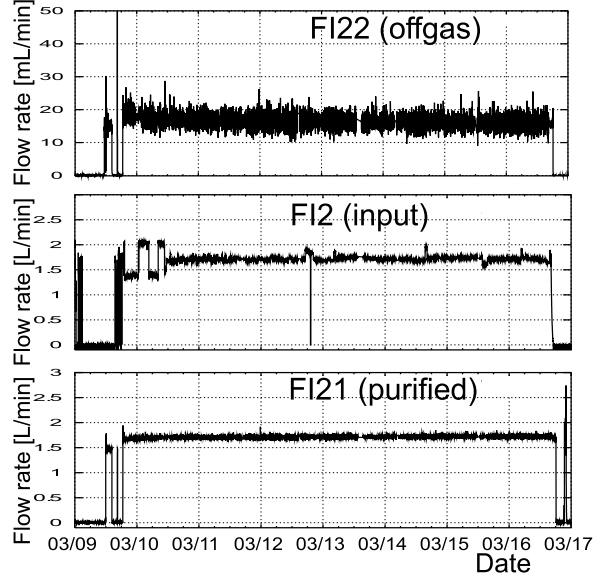


Fig. 5. Time variation of flow rate of off-gas xenon (upper figure), and input (middle) and purified xenon (lower).

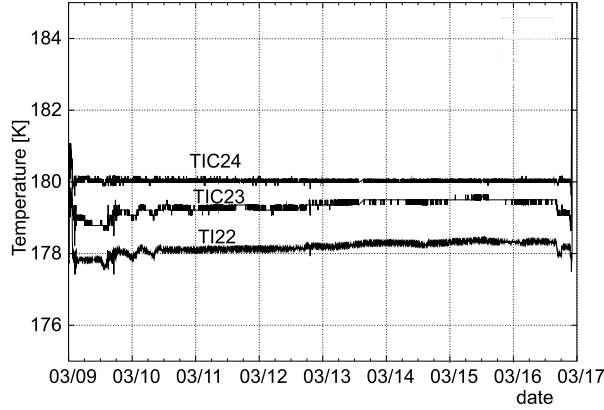


Fig. 6. Temperature variation of condenser, (TI22), reboiler (TIC24) and center position in the tower (TIC23).

#### 4.1 Krypton concentration in xenon feed

The Kr concentration in the original xenon sample was evaluated by scintillation measurement in a prototype detector for the XMASS experiment[1]. The original xenon sample (100 kg) was placed in a 30 L chamber, and scintillation light was detected using 54 low-background photomultipliers[10]. The background spectrum was measured in December 2003, and the background rate around 200–300 keV was estimated to be  $(2 \sim 3) \times 10^{-2}$  /kg/keV/day. This background level corresponds to a Kr concentration of  $\sim 3 \times 10^{-9}$  mol/mol [11], assuming  $^{85}\text{Kr}$  is the main source.

## 4.2 Measurement of off-gas xenon

The Kr concentration of the off-gas xenon was measured on March 23, 2004, by a method employing gas chromatography (GC) and a photoionization detector (PID) connected to the GC column. Xe and Kr were separated by GC according to the difference in their diffusion speeds, and the ion count was measured when the Kr atoms arrived at the PID. The GC system for this experiment was a GC-263-50 (Hitachi Co.) with a separation column consisting of a SUS tube of 3 mm inner diameter and 2 m length, which was filled with MS-13X molecular sieves (30/60 mesh). In order to calibrate the system, a sample gas consisting of  $1 \times 10^{-6}$  Kr, 1% Xe and 99% helium (1 ppm Kr gas) was measured using this setup, and the count of Kr at the PID is shown in Fig. 7(a) for a gas sample of 5 mL. The integrated count rate for the Kr

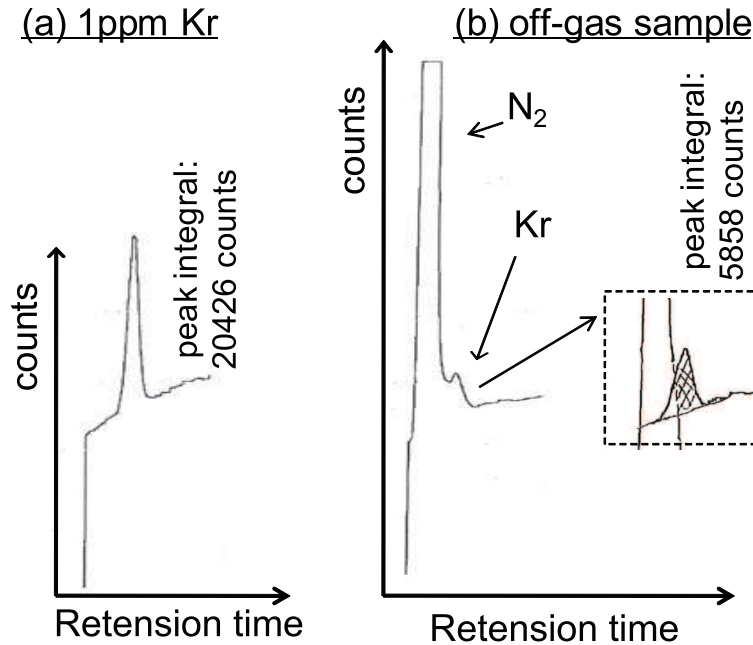


Fig. 7. Kr count by PID detector. The horizontal axis represents travel time through the GC column. (a) Count rate for calibration gas consisting of  $1 \times 10^{-6}$  mol/mol Kr, 1% Xe and 99% helium. (b) Count rate for the off-gas sample.

peak was 20,426. The off-gas measurement is shown in Fig. 7(b) for a sample of 5 mL. The large peak in front of the Kr peak is due to the N<sub>2</sub> component in the off-gas. As described in the previous section, the off-gas was collected by a cold trap method using a collection bottle immersed in liquid nitrogen. Unfortunately, there was a small leak at the endcap of the off-gas collection bottle. The Kr concentration in the off-gas was evaluated by subtracting the tail of the N<sub>2</sub> contribution as shown in the figure, and the resulting integral count rate of Kr in the off-gas was 5858. Normalization of this value based on the calibration gas gave a Kr concentration in the off-gas of  $(3.3 \pm 1.0) \times 10^{-7}$

mol/mol. The error was estimated by evaluating the subtraction of the N<sub>2</sub> background.

### *4.3 Measurement of krypton concentration in purified xenon*

A highly sensitive counting method was needed to measure the Kr concentration in the purified Xe, because the concentration was expected to be as low as  $1 \times 10^{-12}$  mol/mol. The measurement described below was carried out in September 2004. We first describe the principle of the counting method.

The most sensitive method of gas component measurement which can be applied to the measurement of Kr concentration is API-MS (atmospheric pressure ionization mass spectroscopy). In this method, a sample gas can be introduced at near atmospheric pressure, which enables large amounts of gas to be loaded and consequently allows highly sensitive measurements. The gas that carries the sample into the API-MS system (the carrier gas) must have a greater ionization energy than the target elements. The carrier gas mixed with the sample gas is ionized at the first stage (at this time, most of the ionized gas is carrier gas), and a charge exchange interaction in the next stage transfers charge from the carrier gas to the target elements. The ionized elements are then extracted and measured using a mass spectrometer. We used helium as a carrier gas, because the ionization energies of He and Kr are 24.6 eV and 14.0 eV, respectively. Since the ionization energy of Xe (12.3 eV) is lower than that of Kr, Xe must be removed before introducing the sample into the API-MS. We used a GC technique for this purpose. In order to load a large amount of the sample gas, we used a concentration method, as detailed later.

Figure 8 shows the setup for high-sensitivity Kr measurement. First, the sample Xe gas was transferred to a 5 mL sample volume. The 5 mL sample was then transferred to the GC system using helium gas. The GC system used for this was GC-8APT (Shimadzu Co.) and the separation column consisted of a SUS tube of 3 mm inner diameter and 2 m length, which was filled with MS-5A molecular sieves (30/60 mesh). When the separated Kr arrived at the output line of the GC, the line was connected to a metal filter (Nihon Seisen Co., pore size 0.003  $\mu\text{m}$ ) which was cooled by liquid nitrogen, and the Kr was trapped by the metal filter. The trapping efficiency was evaluated based on the results obtained for the calibration gas, and was found to be as high as 80%. The processes described so far were repeated 100 times (concentration process), which enabled loading 500 mL ( $5 \text{ mL} \times 100$  times) of the sample gas. After concentration, the metal filter was warmed to room temperature by removal of the liquid nitrogen vessel. The helium carrier gas was then used to transfer the Kr trapped in the metal filter to the API-MS. Another GC system was placed just in front of the API-MS to remove elements other than Kr. The

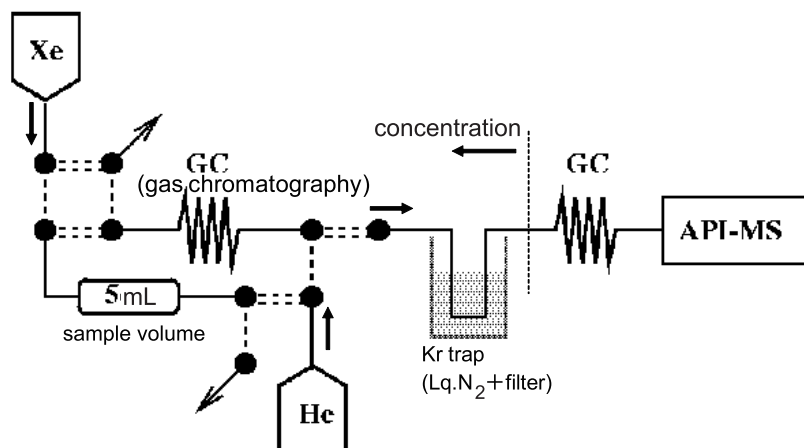


Fig. 8. Setup of high-sensitivity measurement of Kr in xenon gas.

GC system used at this point had a separation column consisting of a SUS tube of 3 mm inner diameter and 2 m length which was filled with MS-13X molecular sieves (30/60 mesh). The API-MS apparatus was API-200 (VG Gas Analysis Systems Ltd). The count rate of the processed and concentrated Kr sample is shown in Fig. 9(a). The M/Z value (the mass number of the element

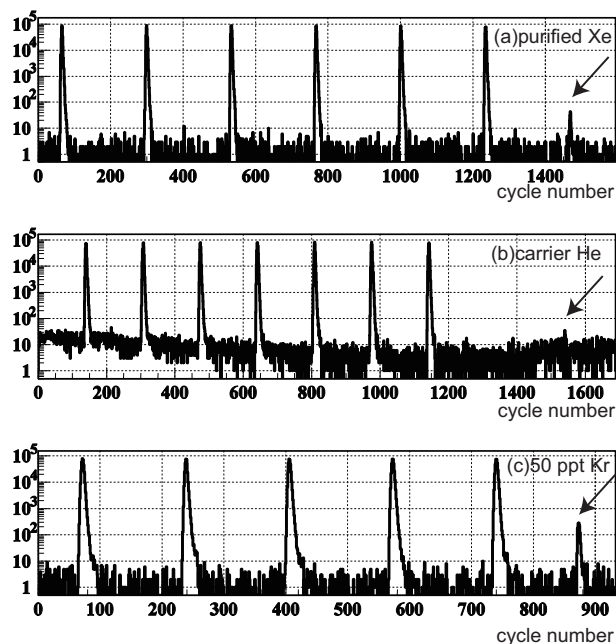


Fig. 9. Kr count rate measured by API-MS for (a) purified Xe gas, (b) He carrier gas, and (c) 50 ppt Kr calibration gas. Kr counting for each gas was conducted at the cycle marked by the arrow. The high peaks appearing periodically before the real measurements represent injections of 1 ppm Kr calibration gas, which is composed of  $1 \times 10^{-6}$  mol/mol Kr, 1% Xe and 99% He.

divided by the charge) was set to 84 in this measurement in order to count  $^{84}\text{Kr}^+$  ions. In order to check the stability of the API-MS system, a standard mixed gas composed of  $1 \times 10^{-6}$  Kr, 1% Xe and 99% He (1 ppm Kr gas) was injected before the introduction of the sample gas. The six peaks before cycle number 1300 in Fig.9(a) are due to the injection of the 1 ppm Kr gas. The real Kr signal of the purified Xe was counted at around cycle number 1470. Figure 10 shows a closer view of the region around the signal. The signal count

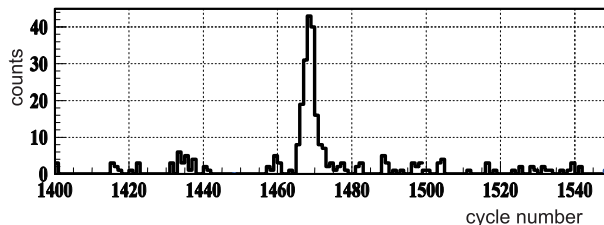


Fig. 10. Kr count rate in purified Xe. Expanded view of Fig. 9 in the signal region.

was defined as the integral counts within  ${}_{-20}^{+30}$  cycles of the peak, and this was calculated to be  $219 \pm 14.8$ . The background count of the API-MS was evaluated using the counts 50 cycles before and 50 cycles after the signal region; the value obtained was  $0.70 \pm 0.08$  counts/cycle. After subtracting the background contribution, the true Kr count of the purified Xe was calculated to be  $184.0 \pm 15.8$ . In order to estimate Kr contamination in the carrier gas, the concentration process was repeated only using the He carrier gas (i.e. without introducing the 5 mL xenon sample during each cycle). The API-MS count for the He carrier gas is shown in Fig. 9(b). Similarly, in order to evaluate the overall counting efficiency, which incorporates the collection efficiency of Kr and the counting efficiency of the API-MS system, a calibration gas containing  $5 \times 10^{-11}$  mol/mol Kr (50 ppt Kr) was processed using the same method; its count rate is shown in Fig. 9(c). The initial signal counts, background count rates and true signal counts (with background rate subtracted) for the purified Xe sample, the He carrier gas and the 50 ppt Kr gas are summarized in Table 1. The counting rates of the 1 ppm Kr gas for the He carrier gas and the 50 ppt Kr calibration gas measurements were 92 % and 88 % of that of the purified Xe gas measurement, respectively, and this factor is corrected in obtaining the true signals in Table 1.

-	Purified Xe	He carrier gas	50 ppt Kr
Signal	$219 \pm 14.8$	$409 \pm 22.2$	$1235 \pm 35.1$
BG count/cycle	$0.70 \pm 0.08$	$6.41 \pm 0.25$	$1.16 \pm 0.12$
True signal(S)	$184.0 \pm 15.8$	$95.6 \pm 25.8$	$1341.7 \pm 40.7$

Table 1

Signal counts, background count rates and true signal counts for purified Xe, He carrier gas, and 50 ppt Kr gas. The true signal is  $(\text{signal} - \text{BG}/\text{cycle} \times 50\text{cycles})/\text{factor}$ , where the *factor* is the relative counting rate of the 1 ppm Kr gas.

The Kr concentration of the purified Xe was calculated using the following formula:

$$\text{Kr concentration} = \{(\text{Purified Xe}) - (\text{He carrier gas})\} \times \frac{5 \times 10^{-11}}{(50 \text{ ppt Kr})}$$

where the values in round parentheses are the true signal counts given in Table 1. The value obtained for Kr concentration was  $(3.3 \pm 1.1) \times 10^{-12}$  Kr/Xe [mol/mol].

## 5 Conclusion

A distillation system for removing Kr from Xe down to a concentration of  $\sim 10^{-12}$  Kr/Xe[mol/mol] was developed. The system was designed to reduce Kr concentration by three orders of magnitude with 99% Xe collection efficiency (i.e., the amount of Xe rejected is only 1%) and with a process speed of 0.6 kg Xe/h. This distillation system was used to purify 100 kg xenon gas containing  $3 \times 10^{-9}$  Kr mol/mol. The off-gas was found to have a Kr concentration of  $(3.3 \pm 1.0) \times 10^{-7}$  mol/mol, which is consistent with the transfer of the majority of Kr in the original Xe sample to the off-gas. The Kr concentration of the purified Xe was measured as  $(3.3 \pm 1.1) \times 10^{-12}$  Kr/Xe[mol/mol] using a gas chromatography apparatus and a API mass spectrometer. These measurements confirmed that the distillation system can reduce the amount of Kr in xenon gas by up to three orders of magnitude. The achieved Kr concentration satisfy the level required for the next generation of dark matter experiments.

## 6 Acknowledgements

We gratefully acknowledge the cooperation of Kamioka Mining and Smelting Company. This work was supported by the Japanese Ministry of Education, Culture, Sports, Science and Technology, and a Grant-in-Aid for Scientific Research.

## References

- [1] Y. Suzuki *et al.*, ICRR-REPORT-465-2000-9, hep-ph/0008296.
- [2] J. Angle *et al.*, Phys. Rev. Lett. 100 (2008) 021303.
- [3] R. Bernabei *et al.*, Phys. Lett. B436 (1998) 379.

- [4] G. J. Alner *et al.*, *Astropart. Phys.* 28 (2007) 287.
- [5] S. Mihara *et al.*, *Cryogenics*. 44 (2004) 223.
- [6] Y. Igarashi *et al.*, *Journal of Environmental Radioactivity* 50 (2000) 107.
- [7] P. Cauwels *et al.*, *Radiation Physics and Chemistry* 61 (2001) 649.
- [8] A. I. Bolozdynya *et al.*, *Nucl. Instrum. Methods A* 579 (2007) 50.
- [9] W. L. McCabe and J. C. Smith, *Unit Operations of Chemical Engineering*, 3rd Edition, McGraw-Hill (1976).
- [10] XMASS collaboration, S. Moriyama *et al.*, *Proceedings of the fourth international workshop on neutrino oscillation and their origin*, World Scientific, pp. 364-371 (2003).
- [11] XMASS collaboration, T. Namba *et al.*, *Proceedings of the fifth international workshop on neutrino oscillation and their origin*, World Scientific, pp. 387-395 (2004).